CONCENTRATION ASSIMILATION INTO WIND FIELD MODELS FOR DISPERSION MODELING

Anke Beyer-Lout*, George S. Young, Sue Ellen Haupt
The Pennsylvania State University, University Park, Pennsylvania

1. INTRODUCTION

Transport and dispersion models are important tools for predicting the impact of a chemical, biological, radiological, or nuclear (CBRN) release. In an emergency situation local authorities require a fast and accurate forecast of the dispersion of the harmful contaminant so as to alert or evacuate the residents of the threatened area. To produce such forecasts, transport and dispersion models need accurate information on source characteristics and various meteorological fields. The source information, i.e. source location and strength, is complicated to determine. In contrast, meteorological information, such as wind direction and speed is routinely available from land surface stations or numerical weather prediction (NWP) models. The meteorological data is, however, likely to be sparse or inaccurate because of low monitoring network densities, observational errors and the finite grid resolution of NWP models. Therefore, emergency managers need to use all of the data available, both meteorological and concentration data, to produce a better forecast of the dispersion of the hazardous contaminant. Data assimilation provides a methodology for this class of problem. With data assimilation we can combine all available multivariate information into a unified description of the coupled weather and concentration system and so improve the forecast model performance.

The current study compares the performance of the conventional data assimilation techniques used in NWP applied in an unconventional framework introducing the assimilation of both wind and concentration observations. For this purpose a simple two-dimensional wind model is coupled with a basic transport and dispersion model. The performance of the data assimilation techniques is assessed through a series of identical twin experiments. After the assimilation period, wind and concentration forecasts are compared for different

observational network setups and densities. The goal is to find a data assimilation method that improves the forecast not only of the hazardous contaminant but also of the wind field. Moreover, it must do so in a timely enough fashion to be of use in CBRN emergency situations.

The performance of atmospheric transport and dispersion models highly depends on the quality of the driving meteorological fields. Thus, there are several approaches to improve the concentration forecast. Davakis et al. (2007) used a multivariate optimal interpolation scheme (Gandin 1963) to assimilate wind velocity observations into a diagnostic meteorological model. Davakis reported an improvement in the performance of the transport and dispersion model driven by the wind field output of this diagnostic model. Other approaches directly assimilate concentration observations into the dispersion model. Constantinescu et al. (2007) used an air quality model and the ensemble Kalman filter to improve the concentration fields of both directly observed and unobserved chemical species. Daley (1995) used a different approach to improve the performance of transport and dispersion models, showing that it is possible to recover the wind field directly from chemical constituent observations. Daley used the extended Kalman filter and a one dimensional constituent transport model coupled to a linear wind model. The forecast performance was improved, provided that the concentration observations were sufficiently accurate and frequent. Stuart et al. (2007) studied the ensemble Kalman filter in the context of a two dimensional sea breeze model directly coupled with chemical tracer transport. The ensemble Kalman filter did not only improve the forecast of the constituent but also the wind field.

These studies demonstrate that concentration assimilation can be implemented successfully in coupled dispersion and wind model systems. However, these studies worked with a continuous concentration field and so were subject to computational dispersion of their advective scheme, and to additional computational cost compared to the entity based concentration assimilation system discussed here.

* *Corresponding author address:* Anke Beyer-Lout,
Dept. of Meteorology, 503 Walker Building,
Pennsylvania State Univ., University Park, PA 16802-5013; e-mail: aub166@psu.edu.

Emergency response situations place harder constraints on dispersion models than air quality applications (Fast et al. 1995). In a CBRN release the constituent plume or puff is more localized. Most of the observation stations report zeros. Emergency managers are also under a time constraint. The current study uses data assimilation to try to improve the forecast not only of a hazardous contaminant but also of the wind field under the given constraints.

In Section 2 the model used as a test bed will be discussed. The experimental setup and the data characteristics are provided. Section 3 lays out the main characteristics of the data assimilation techniques to be tested. Section 4 details the results. The conclusions and implications are discussed in Section 5.

2. EXPERIMENTAL DESIGN

The Gaussian Puff model (Arya 1999) for an instantaneous release suggests itself for initial testing of the different assimilation techniques as it is the most basic time-dependent ensemble-averaged dispersion model. It requires a minimum of input information, is easily implemented, and treats the release as a computationally efficient single entity. To drive the Gaussian Puff model a reduced gravity two dimensional shallow water model (Holton 1992) is chosen, again due to its simplicity and straightforwardness. TusseyPuff couples these two model elements and provides a basic but comprehensive test environment.

2.1. *The TusseyPuff System*

The shallow water model is based on the following equations of motion:

$$\frac{\partial u}{\partial t} + u\frac{\partial u}{\partial x} + v\frac{\partial u}{\partial y} = -g'\frac{\partial h}{\partial x} - \frac{1}{\rho h}\tau_{Bx} \quad (1)$$

$$\frac{\partial v}{\partial t} + u\frac{\partial v}{\partial x} + v\frac{\partial v}{\partial y} = -g'\frac{\partial h}{\partial y} - \frac{1}{\rho h}\tau_{By} \quad (2)$$

$$\frac{\partial h}{\partial t} + \frac{\partial}{\partial x}(uh) + \frac{\partial}{\partial y}(vh) = 0 \quad (3)$$

Where, u is the zonal velocity component, v is the meridional velocity component, g' is the reduced gravitational acceleration $g' = g\Delta T/T$, ρ is the density and h is the depth of the fluid layer being modeled. The stress at the bottom of the layer τ_B is parameterized as:

$$\tau_{Bx} = \rho c_D u\sqrt{u^2 + v^2}$$
$$\tau_{By} = \rho c_D v\sqrt{u^2 + v^2}$$
(4)

where c_D is the drag coefficient, taken here to be 0.02.

The model domain spans 9 km x 9 km, with 30 x 30 grid points, yielding a grid spacing of 300 m in both the x- and the y-direction. The mean fluid depth of the layer is chosen to be 500 m, the temperature of the layer T is 300 K and the temperature discontinuity above the layer ΔT is chosen to be 12 K, resulting in a gravity wave speed $U = \sqrt{g'h}$ of approximately 14 ms^{-1}.

A centered in time and centered in space (leapfrog) finite differencing scheme (Pielke 1984) is used to approximate equations (1)-(3). The leapfrog scheme was chosen because it is simple to implement and it is linearly stable (Pielke 1984). All three model variables (u, v and h) are diffused in space as shown in equation (5) (Pielke 1984).

$$u_{x,y}^{\tau+1} = \frac{df(u_{x+1,y}^{\tau+1} + u_{x,y+1}^{\tau+1} + u_{x-1,y}^{\tau+1} + u_{x,y-1}^{\tau+1}) + u_{x,y}^{\tau+1}}{1 + 4df} \quad (5)$$

Furthermore, to prevent time splitting of the solution, every 10 time steps an Asselin time filter (Asselin 1972) is employed. The variables are averaged in time to assure that even and odd time steps remain consistent with each other.

For simplicity, periodic boundary conditions are imposed in both the x and y direction (Pielke 1984). Topography is introduced into the model to create a more diverse and chaotic wind field. The model is initialized with a small fluid height perturbation, the simplest possible mesoscale weather system. Figure 1 shows the shallow water domain with the topography at the initial time.

The Gaussian Puff model computes a concentration field of a dispersed contaminant C, depending on the emission rate Q of the contaminant, the distance between receptor location and the puff center $(x-\bar{x})$ and $(y-\bar{y})$, and the puff spread σ (Beychok 1995).

$$C = \frac{Q}{2\pi H \sigma^2} \cdot \exp\left(-\frac{(x-\bar{x})^2}{2\sigma^2}\right) \cdot \exp\left(-\frac{(y-\bar{y})^2}{2\sigma^2}\right) \quad (6)$$

The puff spread σ is obtained by converting the Pasquill Gifford dispersion coefficients into analytical equations (Beychok 1995). This study uses Turner's equation for σ (McMullen, 1975):

$$\sigma = \exp(I + J \cdot (\ln(X) + K \cdot (\ln(X))^2) \quad (7)$$

where X is the downwind distance to the receptor from the source (in km) and I, J and K are

2

constants that are functions of the atmospheric stability class provided by McMullen. This equation can be written in prognostic form by replacing X with $U \cdot t$ and taking the derivative with respect to t. The puff center location is predicted via advection. The puff advection equations and the equation for the puff spread (7) are discretized with a simple forward in time scheme (Pilke 1984). The resulting model equations are:

$$\bar{x}_{\tau+1} = \bar{x}_{\tau} \Delta t u_{\tau}^{\bar{x}_{\tau}, \bar{y}_{\tau}} \qquad (8)$$

$$\bar{y}_{\tau+1} = \bar{y}_{\tau} \Delta t v_{\tau}^{\bar{x}_{\tau}, \bar{y}_{\tau}} \qquad (9)$$

$$\sigma_{\tau+1} = \sigma_{\tau} + \Delta t J \left(\frac{1}{t} + \frac{2K \ln(Ut)}{t} \right) \cdot$$
$$\exp(I + J \cdot (\ln(Ut) + K \cdot (\ln(Ut))^2) \quad (10)$$

For some data assimilation techniques, such as 4D-Var and the extended Kalman filter, it is necessary to derive the tangent linear model, L, and the adjoint model, L^T (Kalnay 2003). In this study the tangent linear model and the adjoint model are constructed directly from the discretized Tusseypuff model equations. However, using an adjoint model derived from the leapfrog finite difference approximation can cause an oscillatory computational mode resulting from the computational mode of that leapfrog scheme (Sirkes and Tziperman 1997). Therefore, a forward in time – centered in space finite differencing scheme is used and the tangent linear and adjoint model derived will only be approximations. This is sufficient for the scope of this study, because even with an approximate adjoint model successful error propagation can be achieved (Schiller and Willebrand 1995).

The tangent linear and adjoint model equations are derived following Giering and Kaminski (1998). The model equations are first discretized and then nondimensionalized. The nondimensionalization eliminates the need for ad hoc scaling and guarantees a dimensionally consistent adjoint model. The tangent linear equations of the TusseyPuff system can be written in a form such that an initial perturbation evolves in time as follows: $\delta x(t) = L \delta x(t_0)$. The adjoint equations can be put in matrix form in a similar manner, so that a perturbation at time t is propagated backwards in time: $\delta x(t_0) = L^T \delta x(t)$. For the propagation of perturbations over multiple time steps the tangent linear and the adjoint model matrices are multiplied (Kalnay, 2003).

$$L(t_0, t_i) = \prod_{k=i-1}^{0} L(t_k, t_{k+1}) = L_{i-1} L_{i-2} ... L_0 \qquad (11)$$

$$L(t_i, t_0)^T = \prod_{k=0}^{i-1} L(t_{k+1}, t_k)^T = L^T_0 L^T_1 ... L^T_{i-1} \quad (12)$$

2.2. *Data Characteristics*

The TusseyPuff model is used for the data assimilation tests as well as the generation of the observations used for the data assimilation. This identical twin approach is advantageous for a test environment, because it allows us to compare the performance of the different data assimilation schemes with a known 'truth'.

The 'truth' is created by first initializing TusseyPuff with a uniform wind field and a small fluid-height perturbation. After a startup time, during which the model is run forward to achieve consistent velocity and height fields, the contaminant puff is released. The release location was chosen such that the puff trajectory passes through the terrain driven flow.

The resulting data fields are then used to derive the observations used by the data assimilation. A variable number of observation stations are set up randomly in the model domain. The observation stations are located at model grid points, for simplicity, so no interpolation is necessary. The same setup of stations is used for all test scenarios. The sensors record wind velocity and direction, the concentration of the contaminant, or both, depending on the experimental setup, every ten model time steps. A random normal error of 5% of the value is added to the observational fields.

To decrease the size of the forecast error covariance matrix and to minimize computer run time, this study does not assimilate the continuous concentration fields, but rather the four puff parameters, the puff center $\bar{x}$ and $\bar{y}$, the puff spread σ and the puff concentration amplitude Q. These puff parameters are derived from the continuous concentration field by fitting a Gaussian distribution (6) to the observations. While computationally more efficient than assimilating the continuous concentration observations, this approach adds uncertainty when the puff is still small and only a few sensors are hit.

2.3. *Modeling*

Figure 2 shows a diagram outlining the experimental setup. At the time *t=0* the contaminant is released. TusseyPuff assimilates observations over two thirds of the post-spin up run and continues in forecast mode hereafter.

3

Other inputs required by some of the assimilation schemes include the background or forecast error covariance matrix (*P*) and the observation error covariance matrix (*R*). The initial forecast error covariance matrix *P* is assumed to be known from previous forecasts. The observational error, however, has to be estimated. It is assumed to be uncorrelated in space, resulting in a diagonal error covariance matrix *R*. For this study the expected observational error for the velocity fields is fixed in time and estimated to be 10% of the mean value of the observation. The expected errors of the puff parameters are estimated by running an ensemble of 500 different realizations of the puff parameter fitting process described above and comparing these realizations with the truth.

Three different assimilation test scenarios are each tested at varying sensor densities. In the first test scenario only concentration data is assimilated into the TusseyPuff model. In the second test scenario only wind observations are used in the assimilation. For the third test scenario both wind and concentration observations are assimilated.

2.4. *Validation*

The performance of the data assimilation technique is assessed by comparing the model results to the identical twin from which the observations were obtained. To compare the puff trajectories throughout the model run, the root mean squared distance error (RP) of the puff center locations $(\overline{x}, \overline{y})$ is calculated.

$$RP = \sqrt{\frac{1}{T}\sum_{\tau=1}^{T}[(\overline{x}_\tau^t - \overline{x}_\tau^f)^2 + (\overline{y}_\tau^t - \overline{y}_\tau^f)^2]} \qquad (13)$$

where *t* denotes the known 'truth', *f* denotes the forecast and *T* is the number of time steps. The root mean squared error of the final wind forecast (RW) is calculated as follows:

$$RW = \sqrt{\frac{1}{N}\sum_{n=1}^{N}[(u_n^t - u_n^f)^2 + (v_n^t - v_n^f)^2]} \qquad (14)$$

where *t* again denotes the 'truth', *f* denotes the forecast and *N* is the number of grid points. The final concentration forecast is evaluated by calculating the root mean squared error of the final concentration field, using equation (15) and normalizing by the RC value of the model run without data assimilation.

$$RC = \sqrt{\frac{1}{N}\sum_{n=1}^{N}(c_n^t - c_n^f)^2} \qquad (15)$$

The last factor that is taken into account in the evaluation of the performance of the data assimilation methods is the computer run time (CRT).

3. DATA ASSIMILATION

Some of the more advanced, frequently used data assimilation techniques in NWP applications include optimal interpolation (Gandin, 1963), three-dimensional (Sasaki, 1970) and four dimensional variational analysis (3D and 4D-Var) (Lewis and Derber, 1985), extended Kalman filtering (Kalman and Bucy, 1961), ensemble Kalman filtering (Houtekamer and Mitchell, 1998), and Newtonian relaxation (Data Nudging) (Hoke and Anthes, 1976). For our purposes, i.e. the prediction of transport and dispersion of a CBRN release, a flexible assimilation method is needed, not only to improve the accuracy of a forecast with time dependent observational data, but also to use the CBRN concentration data to modify and correct the predicted wind field and vice versa. Both of the Kalman filter techniques, 4D-Var, and Nudging are structured to fit our needs. Therefore, these four data assimilation techniques are discussed below and then tested with the TusseyPuff model.

3.1. *Nudging*

Nudging is a computationally efficient technique that relaxes the model state toward the observations by adding an artificial tendency term to the prognostic equations (Stauffer and Seaman, 1993).

$$\frac{\partial u}{\partial t} + u\frac{\partial u}{\partial x} + v\frac{\partial u}{\partial y} = -g\frac{\partial h}{\partial x} - \frac{1}{\rho h}\tau_{Bx} + \tau(u^o - u) \,(16)$$

Equation (16) provides an example, implemented as the last term in the zonal momentum equation in TusseyPuff. A similar term is added to the meridional momentum equation, the equation for the location of the puff center, the equation for the puff spread σ and the equation for the puff concentration amplitude *Q*. The weighted increment - the difference between observation and forecast - is subtracted at each time step. The relaxation time scale τ, which acts as a proportionality constant for the nudging term, is always positive and is chosen based on scaling arguments so that the nudging tendencies are relatively small compared to the other terms in the prognostic equations (Stauffer and Seaman, 1993). The relaxation timescale is fixed in time at a value of 0.01.

4

Nudging is simple to implement but it can assimilate only those variables that are explicitly modeled, which is a disadvantage when only concentration observations are available. To overcome this limitation and bridge the gap between the concentration observations and the wind model, Feature Extraction is used. At each time step the advective error is estimated from the gradient of the concentration error. The difference in the forecast and the observed concentrations fields is calculated. The strongest gradient in this difference field is scaled and becomes the new wind vector, which is used in the next assimilation step to nudge the TusseyPuff system.

To improve the Nudging performance the relaxation term is spatially weighted with a Cressman weighting function (Cressman, 1959), so that the wind field is nudged not only at one grid point at every assimilation step, but over an area of grid points surrounding each observation. The radius of influence for this weight function is chosen to be one grid point. This provides an area with a diameter of five grid points to nudge over.

3.2. *Kalman Filter*

As with Nudging, the Kalman filter technique assimilates the observations sequentially each time step during the model run (Caya et al, 2005). However, instead of subtracting a fixed fraction of the model error at each assimilation step, the weight for the increment is calculated so it minimizes the forecast error (Kalman and Bucy, 1961).

The filtering process consists of a forecast step and an analysis step (Kalnay, 2003). In the forecast step the TusseyPuff model M produces a forecast x^f with the analysis x^a of the previous time step.

$$x^f(t_i) = M_{i-1}\left[x^a(t_{i-1})\right] \qquad (17)$$

In the analysis step the forecast x^f is updated with the increment $[x_i^o - H(x^f)]$ weighted with the Kalman gain matrix, K. H is the forward-interpolation matrix from the model grid to the observational grid.

$$x^a(t_i) = x^f(t_i) + K_i(x_i^o - H(x^f(t_i))) \qquad (18)$$

The Kalman gain matrix represents the optimal weight that minimizes the analysis error (Kalnay, 2003). The Kalman gain matrix for time i is:

$$K_i = P^f(t_i)H_i^T\left[R_i + H_iP^f(t_i)H_i^T\right] \qquad (19)$$

where R is the observation error covariance and P^f is the forecast error covariance matrix. H_i represents the linearized Jacobian $\partial H/\partial x_i$ which

is identical to H, because H is an identity matrix in TusseyPuff.

Two Kalman filters are tested in TusseyPuff, the extended and the ensemble Kalman filter. These two approaches differ in how the forecast error covariance matrix P is estimated.

3.2.1. *Extended Kalman Filter*

The extended Kalman filter is a variant of the Kalman filter that can be used for nonlinear problems (Miller et al. 1994) and is hence suitable for transport and dispersion applications. Equations (16) – (18) describe the Kalman filtering process (Kalnay 2003). In the extended Kalman filter the forecast error covariance is estimated using the model itself. In the forecast step the forecast error covariance P^a of the previous time step is advanced in time using the tangent linear model L and the adjoint model L^t.

$$P^f(t_i) = L_{i-1}P^a(t_{i-1})L_{i-1}{}^T + Q \qquad (20)$$

A small model error η with the covariance matrix Q is added to the forecast error covariance (Kalnay 2003). The initial forecast error covariance $P^a(t_0)$ is assumed to be known. In the analysis step not only the forecast x^f but also the forecast error covariance matrix P^f are updated.

$$P^a(t_i) = (I - K_iH_i)P^f(t_i) \qquad (21)$$

Depending on the complexity of P, the matrix multiplications in equations (19), (20) and (21) can dominate the computational cost. In our case the matrices P and L have $7 \cdot 10^6$ elements. This makes the extended Kalman filter computationally expensive. The situation would be exacerbated if continuous concentration fields were used instead of the puff parameters.

3.2.2. *Ensemble Kalman Filter*

A promising simplification of the extended Kalman filter is the ensemble Kalman filter (Kalnay, 2003). In this approach an ensemble of data assimilation cycles is carried out simultaneously. The ensemble Kalman filter does not specifically integrate the forecast error covariance forward in time, but instead computes it diagnostically from the spread of the model states across the ensemble (Houtekamer and Mitchell, 1998). Again the filtering process consists of a forecast step and an analysis step. In the forecast step an ensemble of k state vectors $x_k^a(t_{i-1})$ from the previous time step is integrated forward in time.

$$x_k^f(t_i) = M_{i-1}\left[x_k^a(t_{i-1})\right] \qquad (22)$$

This study uses k=5 ensemble members. The ensemble is built manually with different initial wind conditions to span the space of expected uncertainty. The source characteristics stay unchanged across the ensemble. At each forecast step, the forecast error covariance P^f is estimated from the difference of each ensemble member x_k^f and the ensemble mean $\bar{x}^f$.

$$P^f(t_i) = \frac{1}{N-1}\sum_{n\neq 1}^{N}(x_n^f - \bar{x}^f)(x_n^f - \bar{x}^f)^T \qquad (23)$$

In the analysis step the ensemble of forecasts is updated with the increment weighted with the Kalman gain matrix (18).

$$x_k^a(t_i) = x_k^f(t_i) + K_i(x_i^o - H(x_k^f(t_i))) \qquad (24)$$

Again, H is the forward-interpolation matrix from grid to observation network. For the ensemble Kalman filter the expected errors in the observation error covariance R are inflated by a factor of five. This ensures that the ensemble does not converge too quickly to the observations and that the ensemble spread stays sufficiently large.

The ensemble Kalman filter approach avoids complicated matrix operations, because the forecast error covariance is not advanced in time using the tangent linear and adjoint model. So, the ensemble Kalman filter is computationally less expensive than the extended Kalman Filter, even thought the model has to run several times according to the number of ensemble members.

3.2.3. *4D-Var*

Unlike the Kalman filters and Nudging, four-dimensional variational analysis (4D-Var) does not assimilate observations sequentially each time step. 4D-Var tries to find the optimal analysis $x^a(t_0)$ that best fits the background field and all the observations by minimizing a scalar cost function (Lewis and Derber, 1985). The TusseyPuff prediction model is used as a strong constraint. The cost function (37) consists of two parts: the difference between the analysis and the background x^b and a summation over time of the difference between the analysis x_i^a and the corresponding observation x_i^o

$$J(x^a(t_0)) = \frac{1}{2}\left[x^a(t_0) - x^b(t_0)\right]^T B_0^{-1}\left[x^a(t_0) - x^b(t_0)\right]$$
$$+ \frac{1}{2}\sum_{i=0}^{N}\left[\left[H(x_i^a) - x_i^o\right]^T R_i^{-1}\left[H(x_i^a) - x_i^o\right]\right] \qquad (25)$$

where B is the background error covariance, R is the observation error covariance at time i and H is again the forward-interpolation matrix. For the identical twin experiment the cost function is simplified as follows (Li et al 2000):

$$J(x^a(t_0)) = \frac{1}{2}\sum_{i=0}^{N}\left[\left[H(x_i^a) - x_i^o\right]^T R_i^{-1}\left[H(x_i^a) - x_i^o\right]\right]$$
(26)

To minimize this cost function, its gradient is calculated with the help of the adjoint model L^T.

$$\frac{\partial J}{\partial x^a(t_0)} = \sum_{i=0}^{N}\left[L(t_i,t_0)^T H_i^T R_i^{-1}\left[H(x_i^a) - x_i^o\right]\right] \qquad (27)$$

With the initial conditions $x^a(t_0)$ the TusseyPuff model is run forward and the forecast x_i^a and the adjoint model L_i^T are calculated. Throughout the time steps the adjoint model matrices are continuously multiplied according to equation (12). The gradient is calculated at each time step and summed up throughout the model run. With the adjoint model the analysis errors are propagated backward in time to the release time (t=0). Furthermore, the adjoint model connects the concentration field to the wind field, so, as with the Kalman filter, the 4D-Var scheme can assimilate modeled and non-modeled variables. At the end of the model run, a simple steepest descent method is used to compute the change in the initial conditions $x^a(t_0)$ (Kalnay, 2003).

$$\delta x^a(t_0) = -a\frac{\partial J}{\partial x^a(t_0)} \qquad (28)$$

The factor a is chosen arbitrarily. The initial conditions are adjusted accordingly and the procedure is repeated for twenty iterations.

4D-Var is computationally expensive, because the adjoint model matrix L^T is multiplied every time step and the procedure is repeated multiple times.

4. RESULTS

The performance of the data assimilation techniques is studied for the TusseyPuff model using observations from 200, 100, 50 and 10 observation stations randomly located in the model domain. Figure 3 compares the forecast without data assimilation to the identical twin results. It is evident that the initial wind conditions and hence the puff trajectory vary widely. The errors of the run without data assimilation serve as reference values for the following comparisons of data assimilation methods. The root mean squared error of the location of the puff center (RP), the root mean squared error of the final wind

field (RW), the normalized root mean squared error of the final concentration field and the computer run times (CRT) can be found in Table 1.

In the first scenario tested, only concentration data is assimilated into the TusseyPuff model. Table 2 shows the results for the four different data assimilation techniques and for the four different sensor densities.

The most significant improvement of the wind and the concentration field are achieved by the extended Kalman filter. However, the computer run time (CRT) of the extended Kalman filter is approximately ten hours[1], so it may not be applicable in a CBRN emergency response situation on the current platform. This is also the case for 4D-Var with a CRT of over 24 hours. Nudging, with a model run time of only three minutes, is by far the fastest method tested. However, the Nudging technique, while enhancing the concentration prediction, cannot successfully improve the wind forecast for this test scenario. Figure 4 shows the Nudging results for 200 observation stations for all four scenarios. Figure 4a indicates that the final wind forecast shows no improvement over the run without data assimilation (Figure 3). This result occurs because the concentration field provides only one wind observation, but yields an analytic estimate of the entire concentration field via equation (6).

As the number of concentration observations decreases so does the quality of the puff parameter estimates, because there are fewer observations in the puff upon which to base the estimates. With a further decrease in the number of observation stations, the odds of the puff even hitting the sensor begin to fall. Thus, with a sufficiently low observational network density, the puff observations become more and more infrequent, as the chances of the puff hitting a sensor decrease. In the case of ten observation stations, only one observation of the puff is available throughout the whole assimilation period.

The ensemble Kalman filter provides a good compromise between computer run time (CRT) and forecast improvement. For a large number of observation stations the ensemble Kalman filter improves both the concentration and wind forecast considerably with a run time of less than 15 minutes. The ensemble Kalman filter is also not as strongly dependent on the number of observation stations as Nudging, and therefore, may meet the needs of emergency response

---

[1] Computations were performed on a single thread of a 3.2 GHz dual core processor machine running Matlab.

modeling, particularly if implemented in a compiled language on a multiprocessor system.

In the second test scenario, only wind observations are assimilated into the TusseyPuff system. Table 3 provides the errors of the data assimilation runs for the different observation sensor densities. Again, the most significant improvement of the concentration field is achieved by the extended Kalman filter. The extended Kalman filter is not strongly affected by the number of observation stations. Nudging produces the best wind forecast, with the lowest root mean squared error of the wind field (see Figure 4b). The larger wind error of the extended Kalman filter can be explained by the fact that the tangent linear model and the adjoint model do not incorporate topographical effects. Nudging also has the shortest model run time, but the results are again strongly dependent on the number of observation stations. The ensemble Kalman filter performs well, especially for the low observational density. However, the CRT of the ensemble Kalman filter increases compared to the first scenario due to the larger sizes of the observation error covariance matrix and the Kalman gain matrix.

In the third test scenario, both wind observations and puff parameters are assimilated into the TusseyPuff system. Table 4 shows the results for the four different data assimilation techniques, again for the four different sensor densities. For this scenario the concentration and wind observations were taken at the same sensor sites. However, it was found that the performance of the data assimilation techniques is similar in the case of not collocated the observation stations.

As before, the extended Kalman filter produces the best concentration forecast. However, compared to scenario 2, Nudging improves the concentration forecast even further (see Figures 4c and 4d). In combination with the excellent wind forecast for a large number of observation stations and with the shortest model run time, Nudging is computationally the least expensive data assimilation method.

5. CONCLUSIONS

In the event of a CBRN release a fast and accurate dispersion model forecast could help emergency managers in their decision making and save time and lives. Transport and dispersion models would require not only accurate information on source characteristics but also an accurate estimate of the wind fields. Sparse meteorological observations could lead to inaccurate initial wind fields and so produce to an

inaccurate concentration forecast. However, the assimilation of concentration and wind observations into a coupled NWP and dispersion modeling system could improve the forecast model performance.

This approach is demonstrated using a two-dimensional shallow water model coupled with a Gaussian Puff dispersion model to create a test environment for data assimilation techniques. Four continuous data assimilation methods: Nudging, extended Kalman filter, ensemble Kalman filter and 4D-Var are chosen and tested with this TusseyPuff model system in an identical twin experiment. Observations of wind and puff parameters from a different number of randomly located sensors are assimilated into the model and results for multiple data assimilation scenarios are compared.

It is shown that wind and concentration fields can be successfully recovered from measurements of concentration provided that the observations are frequent and dense. So, the results in this study agree with those of Daley (1994). Furthermore, it is shown that assimilation of wind data alone, or in combination with the assimilation of sparse observations of contaminant concentration, can improve the concentration and wind forecast significantly.

The extended Kalman filter performed best throughout all of the tested scenarios. However, this technique is computationally expensive and therefore may not be appropriate for a rapid CBRN emergence response system. The ensemble Kalman filter and Nudging display good results, in both the error values and the computer run time and are therefore likely candidates for a CBRN emergency response system. Nudging the coupled model proved especially useful when only wind or a combination of wind and concentration data are available. The ensemble Kalman filter provides promising results when only concentration observations are available.

Before the assimilation of concentration and wind data into a coupled NWP and dispersion system can become a routine tool in CBRN emergency situations additional tests with more sophisticated models are necessary. Two intermediate steps present themselves for improving either one or the other of the models. First the two-dimensional multi-Puff model developed by Reddy et al. (2007) will be coupled with the 2-D shallow water model presented here to test the data assimilation techniques. The second approach involves coupling the basic Gaussian Puff model to a full mesoscale model.

Ultimately the most effective and efficient data assimilation methods should be tested in a coupled model including both a multi-puff dispersion component and a full mesoscale model. However, at that level of complexity, computational efficiency is likely to be critical.

6. REFERENCES

Arya, S.P., 1999: Air Pollution Meteorology and Dispersion. Oxford University Press, Oxford.

Asselin, R., 1972: Frequency filter for time integrations. *Mon. Wea. Rev*, 100, 487-490.

Beychok, M.R., 1995: *Fundamentals of stack gas dispersion.* 4rd Edition, California, USA, p. 50 – 56.

Caya, A., J. Sun, and C. Snyder, 2005: A Comparison between 4D Var and the Ensemble Kalman Filter Technique for Radar Data Assimilation. *Mon. Wea. Rev.*, **133**, 3081-3093.

Constantinescu, E.M., A. Sandu, T. Chai, G.R. Carmichael, 2007: Assessment of ensemble-based chemical data assimilation in an idealized setting. *Atmos. Environment* **41**, 18-36

Cressman, G.P., 1959: An Operational Objective Analysis System. *Mon. Wea. Rev*, 10, 367-374.

Daley, R., 1991: *Atmospheric Data Assimilation.* Cambridge University Press, Cambridge, 457 pp.

Daley, R., 1995: Estimating the wind field from chemical constituent observations: experiments with a one-dimensional extended Kalman filter. *Mon. Wea. Rev*, 123, 181-198

Davakis, E., S. Andronopoulos, I. Kovalets, N. Gounaris, J.G. Bartzis, S.G. Nychas, 2007: Data assimilation in meteorological pre-processors: Effects on atmospheric dispersion simulations. *Atmos. Environment* **41**, 2917-2932

Fast, J.D., B.L. O'Steen, and R.P. Addis, 1995: Advanced Atmospheric Modeling for Emergency Response. *J. Appl. Meteor.*, **34**, 626-648.

Gandin, L. S., 1963: Objective analysis of meteorological fields. Gidrometeor. Isdaty., Leningrad. [Israel Program for Scientific Translations, Jerusalem, 1965, 242 pp.]

Giering R. and T. Kaminski. 1998: Recipes for adjoint code construction. *ACM Trans. Math. Software*, **24**, 437—474.

Hoke, J.E., and R.A. Anthes, 1976: The Initialization of Numerical Models by a Dynamic Initialization Technique. *Mon. Wea. Rev.*, **104**, 1551-1556.

Holton, J.R. 1992: *An introduction to dynamic meteorology*. Volume 48 of International Geophysics Series. 3rd edition, Academic Press.

Houtekamer, P.L., and H.L. Mitchell, 1998: Data Assimilation Using an Ensemble Kalman Filter Technique. *Mon. Wea. Rev.*, **126**, 796-811.

Kalman, R., and Bucy, R., 1961: New results in linear prediction and filtering theory. Trans. AMSE, *J. Basic Eng.*, **83D**, 95–108.

Kalnay, Eugenia, 2003: *Atmospheric Modeling, Data Assimilation and Predictability*. Cambridge University Press, Cambridge, 136-204.

Lewis, J.M., and J.C. Derber, 1985: The use of adjoint equations to solve a variational adjustment problem with advective constraints. *Tellus*, **37**, 309-327.

Li, Z., I.M. Navon and Y. Zhu, 2000: Performance of 4D-Var with Different Strategies for the Use of Adjoint Physics with the FSU Global Spectral Model. *Mon. Wea. Rev.*, **128**, 668-688.

McMullen, R.W., 1975: The change of concentration standard deviations with distance. *JAPCA* October 1975.

Miller, R.N., M. Ghil, and F. Gauthiez, 1994: Advanced Data Assimilation in Strongly Nonlinear Dynamical Systems. *J. Atmos. Sci*, **51**, 1037-1056.

Pielke, R.A., 1984: *Mesoscale Meteorological Modeling*. 1st Edition, Academic Press, New York.

Reddy K.V.U., Y. Cheng, T. Singh, P.D. Scott, 2007: Data Assimilation in Variable Dimension Dispersion Models using Particle Filters. *The 10th International Conference on Information Fusion*, Quebec, Canada

Sasaki, Y., 1970: Some basic formalisms in numerical variational analysis. *Mon. Wea. Rev.*, **98**, 875-883.

Schiller, A. and J. Willebrand, 1995: A technique for the determination of surface heat and freshwater fluxes from hydrographic observations, using an approximate adjoint ocean circulation model. *J. Mar. Res.,* **53,** 433-451.

Sirkes, Z. and E. Tziperman, 1997: Finite Diffrernce of Adjoint or Adjoint of Finite Difference? *Mon. Wea. Rev.*, **125**, 3373-3378.

Stauffer, D.R., and N.L. Seaman, 1993: Multiscale Four-Dimensional Data Assimilation. J. *Appl. Meteor.*, **33**, 416-434.

Stuart, A.L., A. Aksoy, F. Zhang, J.W. Nielsen-Gammon, 2007: Ensemble-based Data Assimilation and targeted Observation of a Chemical Tracer in a Sea Breeze Model. *Atmos. Environment* **41**, 3082-3094

7. FIGURES AND TABLES
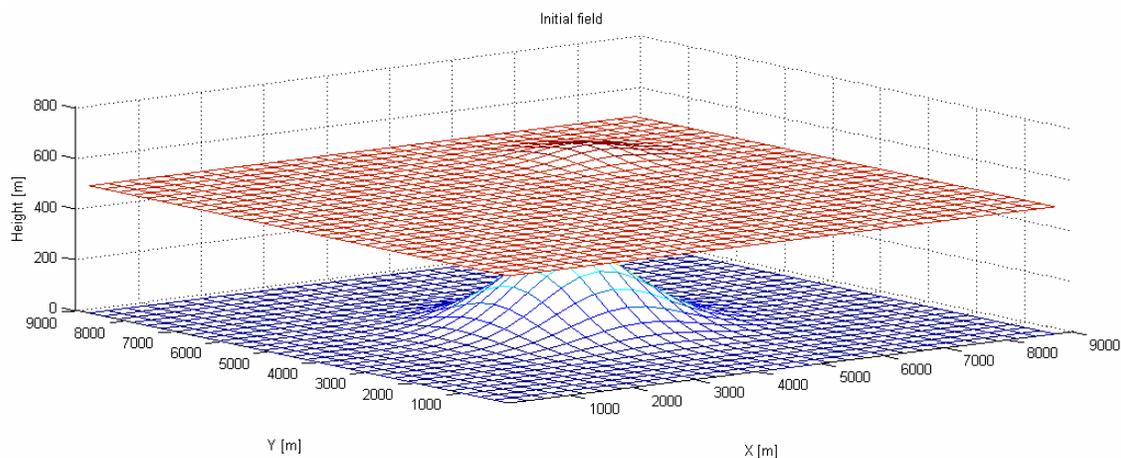
Figure 1: Topography and initial fluid height of the two dimensional shallow water model.
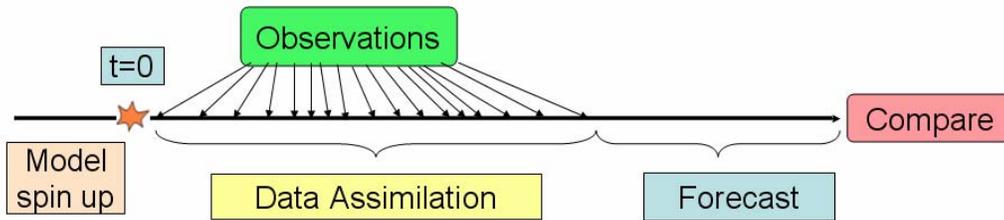
Figure 2: Diagram describing the experimental setup.
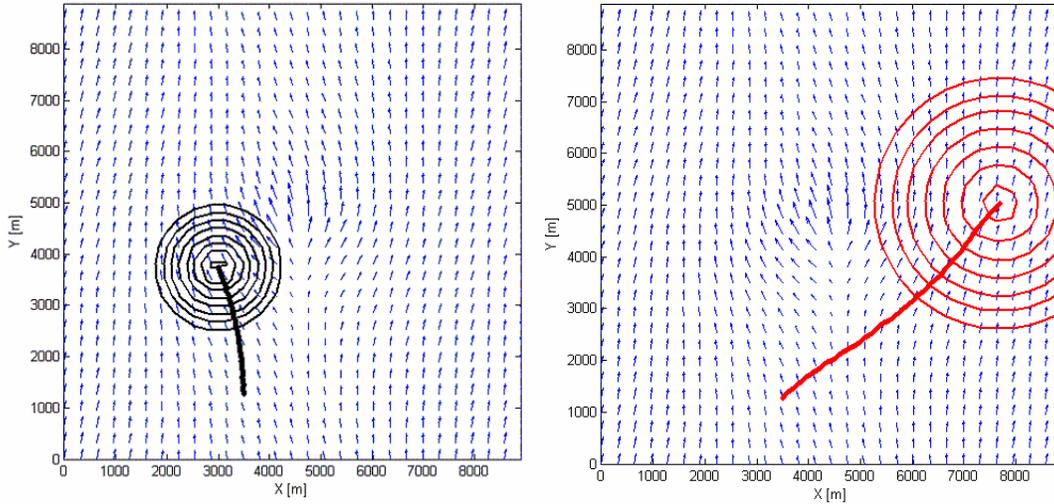
Figure 3: Wind field (arrows), puff concentration field (contours) and puff trajectory of the TusseyPuff model run without data assimilation (left) and the 'truth' model run (right).
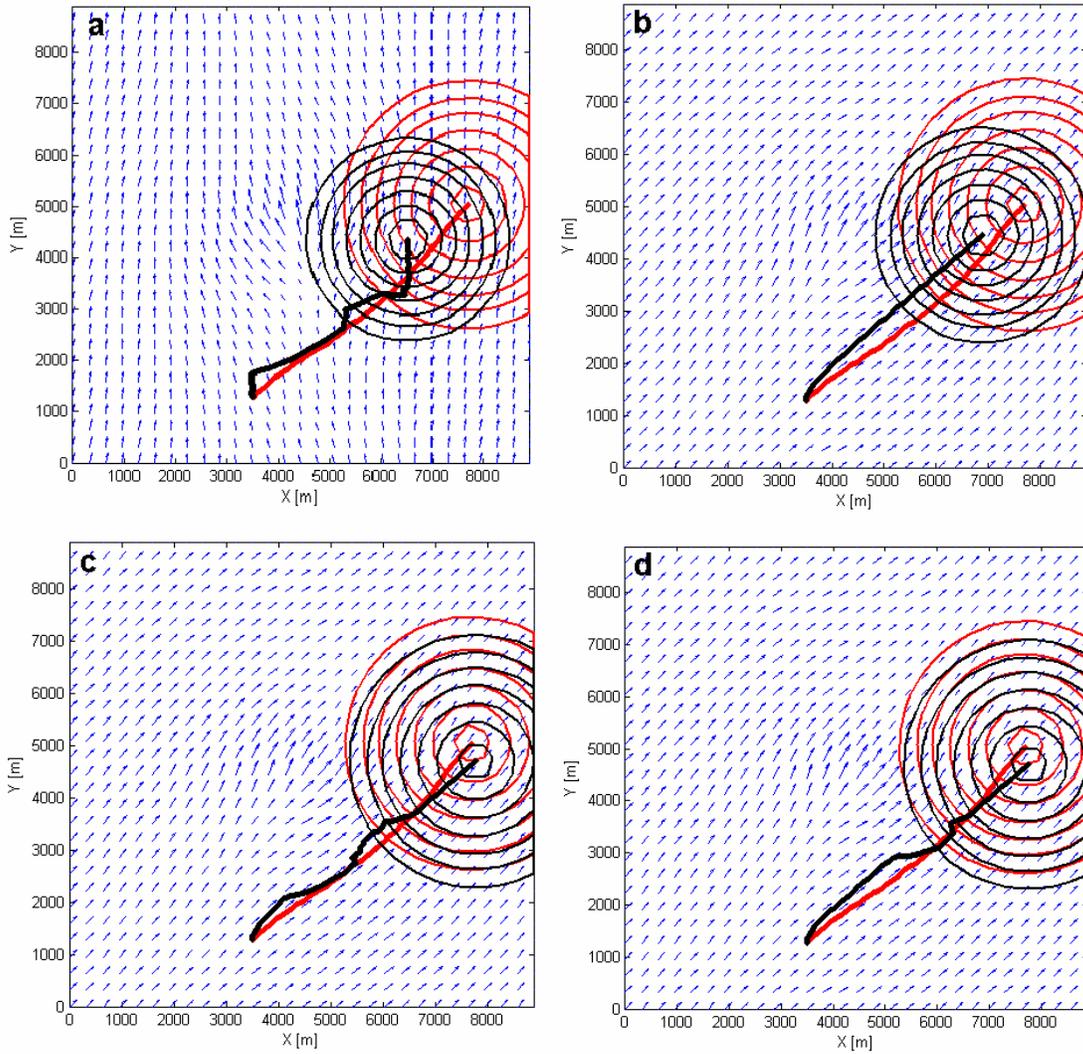
Figure 4: Comparison of the Nudging results (black) to the known 'truth' (red): final wind forecast (blue arrows), final concentration forecast (contours) and puff trajectories (line) for assimilation of concentration data (a), assimilation of wind data (b), assimilation of concentration and wind data from collocated sensors (c) and assimilation of concentration and wind data measured at different locations (d)

Table 1: Error values of the forecast without data assimilation

RP [m]	RW [ms^{-1}]	RC	CRT
2725	0.54	1.0	121 s

Table 2 Summary of the results for scenario 1: assimilation of concentration data into TusseyPuff

# of obser-vation stations	Nudging			Extended Kalman Filter			Ensemble Kalman Filter			4D-Var[2]		
	RP [m]	RW [ms^{-1}]	RC	RP [m]	RW [ms^{-1}]	RC	RP [m]	RW [ms^{-1}]	RC	RP [m]	RW [ms^{-1}]	RC
200	558	0.54	0.70	443	0.28	0.41	327	0.32	0.19	2534	0.53	0.95
100	1480	0.54	0.83	508	0.27	0.50	303	0.30	0.25	2671	0.54	0.97
50	1225	0.54	0.67	1682	0.42	0.93	975	0.40	0.71	2706	0.54	0.97
10	2641	0.54	1.11	2509	0.54	0.98	1254	0.54	0.94	2710	0.53	0.99
CRT	133 s			51700 s			700 s			322400 s		

Table 3 Summary of the results for scenario 2: assimilation of wind data into TusseyPuff

# of obser-vation stations	Nudging			Extended Kalman Filter			Ensemble Kalman Filter			4D-Var		
	RP [m]	RW [ms^{-1}]	RC	RP [m]	RW [ms^{-1}]	RC	RP [m]	RW [ms^{-1}]	RC	RP [m]	RW [ms^{-1}]	RC
200	456	0.01	0.41	34	0.04	0.01	127	0.11	0.25	1984	0.38	0.91
100	653	0.02	0.56	35	0.04	0.01	121	0.11	0.23	2453	0.44	0.98
50	1008	0.04	0.72	33	0.04	0.01	146	0.11	0.27	2623	0.51	0.98
10	1576	0.25	0.79	61	0.04	0.01	144	0.11	0.23	2751	0.54	1.00
CRT	140 s			61300 s			5500 s			342500 s		

Table 4 Summary of the results for scenario 3: assimilation of concentration and wind data into TusseyPuff

# of obser-vation stations	Nudging			Extended Kalman Filter			Ensemble Kalman Filter			4D-Var		
	RP [m]	RW [ms^{-1}]	RC	RP [m]	RW [ms^{-1}]	RC	RP [m]	RW [ms^{-1}]	RC	RP [m]	RW [ms^{-1}]	RC
200	206	0.01	0.04	45	0.04	0.01	138	0.11	0.19	2309	0.44	0.94
100	511	0.02	0.32	38	0.04	0.01	116	0.11	0.15	2561	0.47	0.98
50	650	0.04	0.29	45	0.04	0.01	115	0.11	0.21	2623	0.51	0.98
10	1505	0.25	0.81	39	0.04	0.01	135	0.11	0.21	2734	0.54	0.99
CRT	141 s			65100 s			6100 s			355500 s		

---

[2] The 4D-Var results shown are preliminary. The scheme will be re-examined in the future.